Optical-frequency balanced mixer

J. R. Kurz, K. R. Parameswaran, R. V. Roussev, and M. M. Fejer

E. L. Ginzton Laboratory, Stanford University, Stanford, California 94305

Received April 17, 2001

Optical signal processing devices based on quasi-phase-matched three-wave mixing and cascaded three-wave mixing in guided-wave geometries have been demonstrated to operate efficiently at practical pump-power levels. We describe operation of such devices in a balanced mode that allows mixing without wavelength offset and separation of mixed output from pump and signal input without wavelength-selective filters. We present a design for an optical-frequency balanced mixer using quasi-phase-matched, cascaded second-order nonlinear processes. Using this design, we fabricated a balanced mixer in periodically poled lithium niobate waveguides that has the expected linear and nonlinear optical performance.

OCIS codes: 190.4360, 190.4390, 060.4510, 070.6020, 070.4340, 130.2790.

Optical-frequency (OF) mixers based on periodically poled lithium niobate (PPLN) waveguides are becoming an attractive technology for communications applications because of their high speed, linear response, negligible spontaneous-emission noise, and spectral inversion property. Some of the all-optical functions that have already been demonstrated by use of PPLN waveguides include wavelength conversion,[1,2] switching,[3,4] dispersion compensation,[5] Kerr effect correction,[6] 100-Gbit/s optical time-division multiplexing (TDM),[7] and matched filtering for optical code-division multiple access.[8] As currently implemented, the pump, signal, and output waves exit at the same port, requiring spectral filtering for separation of the output from the other waves.

The OF balanced mixer adds an important new functionality for all quasi-phase-matched (QPM) signal-processing devices, including the above-mentioned PPLN devices: conversion without wavelength offset. It makes possible, for example, a TDM demultiplexer that does not shift wavelength, a wavelength converter that unblocks the input channel, and spectral inverters with adjustable (or even zero) wavelength shift. The balanced mixer permits functions in three-wave mixing devices that are analogous to the four-wave mixing functions made possible by a parametric loop mirror configuration with asymmetrically placed dispersive elements.[9] The OF balanced mixer accomplishes these functions by combining appropriately phased periodically poled sections with waveguide interferometer structures and waveguide phase shifters in an integrated nonlinear optical device. In contrast with noncollinear and two-dimensional QPM schemes,[10,11] the OF balanced mixer achieves spatial separation of the nonlinear output with a collinear interaction section for high efficiency.

A QPM OF mixer using cascaded second-order nonlinearity $[\chi^{(2)}:\chi^{(2)}]$ makes use of difference-frequency generation (DFG) between the second harmonic of a (strong) pump at frequency ω_p and a (weak) signal at frequency ω_s to generate a wavelength-shifted output at $\omega_{\text{out}} = 2\omega_p - \omega_s$.[1,12] Together, the QPM second-harmonic generation and DFG mimic a 1.5-μm-band four-wave mixing process. The effective $\chi^{(3)}$ of this $LiNbO_3$ mixer is 10^4 to 10^5 times larger than that of silica glass; -8-dB fiber-to-fiber conversion has been demonstrated with 175 mW of 1.5-μm pump power[1] in a 5-cm-long device. In the low-conversion-efficiency approximation, the converted output (P_{out}) is proportional to the input signal power (P_s) and the square of the pump power[13] (P_p):

$$P_{\text{out}} \approx \frac{1}{4}\, \eta^2 L^4 {P_p}^2 P_s\,. \quad (1)$$

η is the normalized efficiency [the same for second-harmonic generation and near-degenerate DFG, proportional to both the mode overlap between the interacting waves and the material nonlinearity $\chi^{(2)}$] in units of inverse milliwatts times inverse centimeters squared and L is the interaction length. In state of the art devices, with $\eta \approx 50\%/\text{W/cm}^2$ (or $5 \times 10^{-4}\ \text{mW}^{-1}\ \text{cm}^{-2}$) and $L \approx 5.5$ cm, $\eta L^2 \approx 1.5\%/\text{mW}$, and -8-dB fiber-to-fiber conversion can be achieved with only 50 mW of pump power. Given the same interaction length and normalized efficiency, the OF balanced mixer requires twice as much pump power as a standard device for the same level of performance. The balanced mixer incurs this penalty from using two parallel interaction sections, each containing one half of the input signal and pump powers.

In a standard QPM mixing device, the pump, signal, and output waves mix within a single straight waveguide. The three waves exiting the device are easily separable (or distinguishable) only when $\omega_p \neq \omega_s$. This practical limitation implies that spectral filtering is always required for separation of the output from the pump and signal waves. In an optical TDM device, multiplexing or demultiplexing must always be accompanied by wavelength conversion, which, from a system perspective, may be an undesirable side effect. The corresponding problem in the standard wavelength-converter device is that wavelength channels cannot be used simultaneously for input and output, cutting the available bandwidth in half. Similarly, for standard devices spectral inversion of input spectra that span the pump wavelength is difficult.

The OF balanced mixer, like a rf balanced mixer,[14] solves this set of problems by eliminating or separating the residual signal and pump waves from the desired mixed output. Suitably biased waveguide interferometer structures suppress the residual signal

0146-9592/01/161283-03$15.00/0

and pump waves, while the flexibility of quasi-phase matching allows the generated mixed wave to be biased independently. Figure 1(a) illustrates this idea in a Mach–Zehnder configuration with two 50% directional couplers and two outputs. In this interferometer the input signal and pump waves (gray colored) end up at the bar port. Note that the mixing that occurs in the periodically poled sections (represented by gratings) has no effect on the phase of the input waves in the phase-matched, non-pump-depleted case. The phase of the mixer output (dark colored) generated in each arm, however, is set by the phases of the input waves and by the phase of the grating. A π-phase shift between the two gratings aligns the phase of the mixed output in both arms, resulting in its transmission through the cross port, where it is conveniently separated from the residual input. If Y junctions are used in the interferometer instead of directional couplers, an additional π-phase shift is needed in one arm to discard the pump and signal at the output [Fig. 1(b)]; only mixed output then appears at the output port.

The amount of pump and signal rejection that can be achieved with the balanced mixer is limited only by the contrast of its interferometer structure. Given the current state of commercially available Mach–Zehnder modulators, it should be relatively easy to achieve 20 dB of bias-free contrast; if a dc bias is used in a PPLN device, more than 30 dB of contrast should be possible.[15]

For a proof-of-principle demonstration of the balanced mixer function, we fabricated devices based on the design in Fig. 1(b) and shortened the interaction sections to loosen fabrication tolerances at the expense of lower efficiency. These 23-mm-long devices had interferometer arms with only 12-mm-long periodically poled sections, so they were expected to be ~2500 times less efficient than a standard PPLN waveguide device because of the fourth-power length scaling in expression (1). Only the length-normalized efficiency was important for these initial devices, however, since our primary goal was to establish their novel functionality.

The balanced mixers are proton exchanged to an initial depth of 0.7 μm and annealed for 26 h at 325 °C. The waveguide (mask) width is 3.5 μm at the input and output for efficient coupling and is 12 μm in the periodically poled regions. The 14.75-μm grating period phase matches the fundamental modes at 1544 and 772 nm at room temperature. Since the balanced mixer requires two π-phase-shifted grating sections along closely spaced waveguides, narrow (35 μm as measured perpendicular to the k vector) gratings are used. Unlike previous devices, in which millimeter-wide gratings covered multiple waveguides, the balanced mixer demands more-precise alignment between the electric field poling lithography (to define the electrodes) and the waveguide lithography (to create a proton-exchange mask). Experimentally, we find that smaller electrode widths increase poling fidelity, improving device efficiency. Narrower electrodes inhibit the spread of overpoled sections (run-together domains) and reduce the total current needed to pole a wafer. Narrow electrodes show normal nucleation and growth down to widths of 20 μm for periods of ~15 μm; however, at the narrowest widths, nucleation problems occur when the width and edge-to-edge spacing are comparable over large areas.

The Y-junctions in the balanced mixer have 1-mm-long arms with a (full) opening angle of 2.6°. Their transmission was previously measured to be better than 90% at 1550 nm by use of separate devices with a simpler geometry. Efficient nonlinear mixing requires single-mode junction outputs, and hence a small waveguide width (3.5 μm). Since the optimum (noncritical) width for the QPM waveguides is 12 μm, a taper is required for connection of the Y-junction with the mixing section.[16]

The π-phase shift that biases the balanced mixer also depends on the post-Y-junction taper. By delaying the onset of this taper in one interferometer arm [see Fig. 1(b)], we can use the difference in effective index between the 3.5- and 12-μm-wide waveguides to adjust the bias. We fabricated many balanced mixer devices with various taper delay lengths to explore a full range of relative phases between the two arms. Absolute transmission measurements for devices with taper delay lengths ranging from 0 to 500 μm yield the normalized interferometer contrast curve shown in Fig. 2. Each data point represents a unique device. The transmission measurements use a butt-coupled single-mode fiber as an output coupler; the fiber is crucial for separating the weak device transmission at π-phase bias from the rejected input, which appears as an unguided antisymmetric radiation mode. Although more measurements are needed, it appears that the taper delay length needed for a π-phase shift is ~70 μm, somewhat shorter than had been previously suggested by our waveguide modeling. The contrast of this balanced mixer design is higher than 13 dB, presumably limited by the precision of the Y-junction fabrication and matching of the

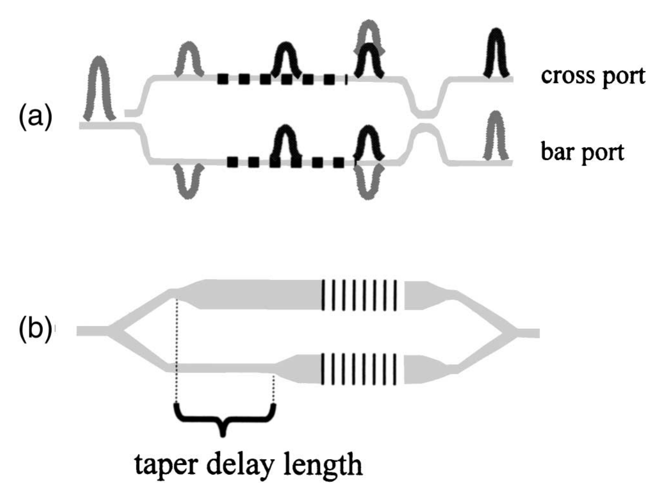

Fig. 1. (a) OF balanced mixer structure using directional couplers. The input waves (gray) exit through the bar port, while a π-phase shift between the gratings in each arm biases the mixer output (black) for transmission through the cross port. (b) Schematic drawing of the demonstration device fabricated by use of Y-junctions; the taper delay length adjusts the relative phase of the lower versus upper arms.

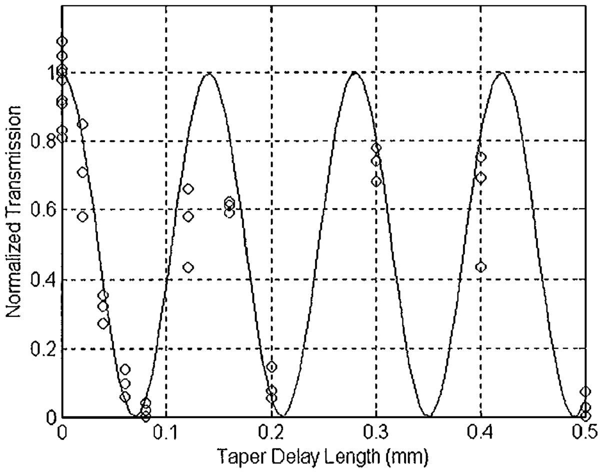

Fig. 2. Measurements of normalized transmission versus taper delay length; each circle corresponds to a unique balanced mixer device. From the fit (solid curve), a taper delay of ~70 μm provides a π-phase shift.

interferometer arms. Any unintentional variations in waveguide fabrication between the two arms can reduce the contrast and change the bias point of the balanced mixer, so much of the spread in the Fig. 2 data probably is due to phase errors in individual devices. Note that the interferometric sensitivity of the balanced mixer places even more stringent tolerances on the waveguide fabrication than the quasi-phase matching does.

We measured the balanced mixer efficiency, using 26 mW of pump power (1552.6 nm) and 21 mW of signal power (1537.1 nm). The pump and signal were combined in the fiber and free-space coupled into the device, which we heated to 90 °C to avoid any possibility of photorefractive effects. The device output, including the generated mixer wave at 1568.4 nm, was measured with an optical signal analyzer. To confirm the nonlinear performance of the interferometer structure, we measured the mixer output power from zero-phase shift (no taper delay section) devices with in-phase gratings in the arms. These devices had a normalized efficiency of 52%/W/cm^2, and one-fourth the output of a standard waveguide with the same grating length, as expected from expression (1). Comparing these results to measurements on devices with out-of-phase QPM gratings, the expected trend was observed for phase biases from 0 to $\pi/2$. Alignment difficulties precluded measurement of such devices with π-phase bias; improved devices that correct for this problem are under development.

In summary, we have demonstrated a design for an optical-frequency balanced mixer in a PPLN waveguide. The proof-of-principle device has the expected mixing efficiency and reasonable output selectivity (greater than 13 dB of input signal and pump rejection). Refinement of the fabrication process and less-critical interferometer designs will increase the contrast and the grating length in future balanced mixer devices. If separate, full 5.5-cm-length SHG and DFG sections with state of the art efficiencies of 1800%/W were connected by a low-loss bend for the second-harmonic wavelength (a technology under development), −3-dB conversion would be possible with 75 mW of pump power.

This research was supported by the Defense Advanced Research Projects Agency through the University of New Mexico Optoelectronic Materials Research Center (Prime MDA972-00-1-0024), U.S. Air Force Office of Scientific Research grant F49620-99-1-0270, the Stanford Graduate Fellowships Program, and Crystal Technology, Inc. J. Kurz's e-mail address is jonkurz@stanford.edu.

References

1. M. H. Chou, I. Brenner, M. M. Fejer, E. E. Chaban, and S. B. Christman, IEEE Photon. Technol. Lett. **11,** 653 (1999).
2. C. Q. Xu, H. Okayama, and M. Kawahara, Appl. Phys. Lett. **63,** 3559 (1993).
3. K. R. Parameswaran, M. Fujimura, M. H. Chou, and M. M. Fejer, IEEE Photon. Technol. Lett. **12,** 654 (2000).
4. H. Kanbara, H. Itoh, M. Asobe, K. Noguchi, H. Miyazawa, T. Yanagawa, and I. Yokohama, IEEE Photon. Technol. Lett. **11,** 328 (1999).
5. M. H. Chou, I. Brener, G. Lenz, R. Scotti, E. E. Chaban, J. Shmulovich, D. Philen, S. Kosinski, K. R. Parameswaran, and M. M. Fejer, IEEE Photon. Technol. Lett. **12,** 82 (2000).
6. I. Brener, B. Mikkelsen, K. Rottwitt, W. Burkett, G. Raybon, J. B. Stark, K. Parameswaran, M. H. Chou, M. M. Fejer, E. E. Chaban, R. Harel, D. L. Philen, and S. Kosinski, in *Digest of Optical Fiber Communication Conference* (Optical Society of America, Washington, D.C., 2000), paper PD-33.
7. S. Kawanishi, M. H. Chou, K. Fujiura, M. M. Fejer, and T. Morioka, Electron. Lett. **36,** 1568 (2000).
8. Z. Zheng, A. M. Weiner, K. R. Parameswaran, M. H. Chou, and M. M. Fejer, in *Ultrafast Phenomena XII: Proceedings of the 12th International Conference*, T. Elsaessner, ed. (Springer-Verlag, Berlin, 2000), p. 159.
9. K. Mori, T. Morioka, and M. Saruwatari, Opt. Lett. **20,** 1424 (1995).
10. A. Chowdhury and L. McCaughan, J. Lightwave Technol. **18,** 688 (2000).
11. A. Chowdhury, S. Hagness, and L. McCaughan, Opt. Lett. **25,** 832 (2000).
12. K. Gallo, G. Assanto, and G. Stegeman, Appl. Phys. Lett. **71,** 1020 (1997).
13. G. P. Banfi, P. K. Datta, V. Degiorgio, and D. Fortusini, Appl. Phys. Lett. **73,** 136 (1998).
14. I. Kása, *Microwave Integrated Circuits* (Elsevier, New York, 1991).
15. P. Hallemeier, K. Kissa, G. McBrien, and T. Horton, paper presented at the 15th Annual National Fiber Optic Engineers Conference (NFOEC), Chicago, Ill., September 26–30, 1999.
16. M. H. Chou, "Optical frequency mixers using three-wave mixing for optical fiber communications," Ph.D. dissertation (Stanford University, Stanford, Calif., 1999).